OXFORD

SOT | Society of Toxicology

www.toxsci.oxfordjournals.org

TOXICOLOGICAL SCIENCES, 151(2), 2016, 365–375

doi: 10.1093/toxsci/kfw047

Advance Access Publication Date: March 8, 2016

Research Article

Subtoxic Alterations in Hepatocyte-Derived Exosomes: An Early Step in Drug-Induced Liver Injury?

Natalie S. Holman,[*,†,‡] Merrie Mosedale,[†,‡] Kristina K. Wolf,[‡,§] Edward L. LeCluyse,[*,‡,2] and Paul B. Watkins[†,‡,1,2]

[*]Curriculum in Toxicology, University of North Carolina at Chapel Hill, Chapel Hill, North Carolina 27599; [†]Division of Pharmacotherapy and Experimental Therapeutics, Eshelman School of Pharmacy, University of North Carolina at Chapel Hill, Chapel Hill, North Carolina 27599; [‡]Institute for Drug Safety Sciences, University of North Carolina at Chapel Hill, Research Triangle Park, North Carolina 27709; and [§]QPS DMPK Hepatic Biosciences, Research Triangle Park, North Carolina 27709

[1]To whom correspondence should be addressed at UNC Eshelman School of Pharmacy, Chapel Hill, NC, 27599. Fax: 919-226-3150. E-mail: paul_watkins@med.unc.edu.

[2]These authors contributed equally to this study.

ABSTRACT

Drug-induced liver injury (DILI) is a significant clinical and economic problem in the United States, yet the mechanisms that underlie DILI remain poorly understood. Recent evidence suggests that signaling molecules released by stressed hepatocytes can trigger immune responses that may be common across DILI mechanisms. Extracellular vesicles released by hepatocytes, principally hepatocyte-derived exosomes (HDEs), may constitute one such signal. To examine HDE alterations as a function of drug-induced stress, this work utilized prototypical hepatotoxicant acetaminophen (APAP) in male Sprague-Dawley (SD) rats, SD rat hepatocytes, and primary human hepatocytes. HDE were isolated using ExoQuick precipitation reagent and analyzed by quantification of the liver-specific RNAs albumin and microRNA-122 (miR-122). *In vivo*, significant elevations in circulating exosomal albumin mRNA were observed at subtoxic APAP exposures. Significant increases in exosomal albumin mRNA were also observed in primary rat hepatocytes at subtoxic APAP concentrations. In primary human hepatocytes, APAP elicited increases in both exosomal albumin mRNA and exosomal miR-122 without overt cytotoxicity. However, the number of HDE produced *in vitro* in response to APAP did not increase with exosomal RNA quantity. We conclude that significant drug-induced alterations in the liver-specific RNA content of HDE occur at subtoxic APAP exposures *in vivo* and *in vitro*, and that these changes appear to reflect selective packaging rather than changes in exosome number. The current findings demonstrate that translationally relevant HDE alterations occur in the absence of overt hepatocellular toxicity, and support the hypothesis that HDE released by stressed hepatocytes may mediate early immune responses in DILI.

Key words: exosomes; drug-induced liver injury; liver-specific RNA; miR-122.

Drug-induced liver injury (DILI) is responsible for significant pre- and post-market drug failures and is the primary cause of acute liver failure in the United States and Europe (Bernal *et al.*, 2010; Ostapowicz *et al.*, 2002; Wilke *et al.*, 2007). DILI, therefore, represents a major economic and clinical challenge for patients, healthcare providers, and pharmaceutical companies. Identification of underlying mechanisms has proved especially difficult as DILI has been associated with hundreds of drugs that elicit a broad spectrum of injuries (Hornby *et al.*, 2014; Hussaini and Farrington, 2014). However, increasing evidence suggests that drug-induced hepatocellular death may often be mediated by immune responses (Adams *et al.*, 2010; Ju and Reilly, 2012; Russmann *et al.*, 2009). For example, human leukocyte antigen genotype is a strong risk factor for DILI associated

with a wide range of drugs, suggesting a role for the adaptive immune system in drug-mediated hepatotoxicity (Urban *et al.*, 2014). In addition, elevations in biomarkers that trigger an innate immune response such as high-mobility group box 1 (HMGB1), and those that are suggestive of immune cell activation including miR-155 and acetylated HMGB1, have been associated with DILI (Antoine *et al.*, 2014; Bala *et al.*, 2012; Fontana, 2014). Furthermore, immune reactions are triggered by hepatocellular danger signals, which can be released in the absence of hepatocyte death and communicate to other cell types as part of a stress response (Uetrecht and Naisbitt, 2013).

Extracellular vesicles (EVs) released by hepatocytes, principally hepatocyte-derived exosomes (HDEs), may constitute one such danger signal (Conde-Vancells *et al.*, 2008; De Maio, 2011; Royo and Falcon-Perez, 2012; Royo *et al.*, 2013). By virtue of their small size (<150 nm), HDE can readily cross through fenestrations in the sinusoidal endothelium and enter the bloodstream (Conde-Vancells *et al.*, 2008), carrying liver-specific contents that are modified during DILI (Wetmore *et al.*, 2010). Clinically relevant alterations in HDE content and quantity have been detected in multiple models of liver injury including viral hepatitis (Zhang *et al.*, 2014), alcoholic hepatitis (Momen-Heravi *et al.*, 2015b), nonalcoholic steatohepatitis (Hirsova *et al.*, 2016), cirrhosis, and hepatocellular carcinoma (Bernal *et al.*, 2010). Moreover, exosomes are immunomodulatory and can carry damage-associated molecular patterns (DAMPs), antigens, and cytokines to recipient cells (Beninson and Fleshner, 2014; De Maio, 2011; Liu *et al.*, 2006; Robbins and Morelli, 2014). In the liver, HDE released by hepatitis C-infected hepatocytes activate dendritic cells and those released during lipotoxicity influence macrophage phenotype (Dreux *et al.*, 2012; Hirsova *et al.*, 2016). Recent experiments have demonstrated that one means by which HDE evoke immune responses is the delivery of functional genetic material such as microRNA (miRNA) and messenger RNA (mRNA). For example, HDE-based RNA species miR-122 and albumin mRNA (*ALB*) have been shown to activate recipient monocytes and fibroblasts, respectively (Momen-Heravi *et al.*, 2015a; Royo *et al.*, 2013).

HDE may play a critical role in the initiation of and response to DILI by transmitting signals of hepatocellular stress that directly or indirectly stimulate an immune response. For HDE to mediate early DILI events, we hypothesized that significant alterations in HDE content and/or number must occur prior to, or in the absence of, overt hepatocellular injury. To better understand the potential of HDE to modulate early immune-driven DILI events, we sought to establish that subtoxic drug-induced HDE alterations were consistent *in vivo* and *in vitro*, and relevant in human DILI. Acetaminophen (APAP) was selected as the model hepatotoxicant due to its well-defined *in vivo* and *in vitro* toxicity profiles. We utilized this prototypical intrinsic hepatotoxicant for verification that the exosomes released by hepatocytes following drug exposure were altered in the absence of overt injury. Although the role of immune reactions in APAP-induced liver injury is controversial, there is recent evidence of induction of immune tolerance in healthy adults that do not develop alanine aminotransferase (ALT) elevations after recurrent therapeutic doses of APAP (Fannin *et al.*, 2015), further supporting selection of APAP as our model toxicant. This finding also suggests that some stress-induced HDE alterations may promote an adaptive response to toxicity rather than an exacerbation of injury.

We therefore evaluated the dose- and time-dependent effects of APAP on HDE-associated RNAs in rats, primary rat hepatocytes, and primary human hepatocytes. Because exosomes in the blood are derived from multiple cell types, exosome-associated liver-enriched *ALB* mRNA and liver-specific miR-122 were assayed as a means to confirm the presence of, and track alterations in, HDE across platforms (Bandiera *et al.*, 2015; Miyamoto *et al.*, 2008).

MATERIALS AND METHODS

Animal Exposures

Male Sprague-Dawley rats (Crl:SD), 7–9 weeks of age, were purchased from Charles River Laboratories and allowed to acclimate in-house for 7–10 days prior to study initiation. Water and food (pelleted PicoLab Rodent Diet 20 [Lab Diet]) were available *ad libitum* during this time. Food was removed during an 18 h fasting period immediately prior to compound administration. APAP (Sigma-Aldrich) was administered in 0.5% (w/v) methylcellulose (Sigma-Aldrich) at 0, 500, or 1400 mg/kg by oral gavage. After dosing, food was provided *ad libitum* until necropsy. Studies were conducted in accordance with the Guide for the Care and Use of Laboratory Animals, and were approved by the Mispro Institutional Animal Care and Use Committee (Mispro Biotech Services, Inc.).

Necropsy and Histology

Rats were euthanized by CO_2 inhalation and subsequent exsanguination at 0, 1, 2, 4, 8, 12, and 24 h post-dose ($n = 6$ per group). Blood was collected in K_2EDTA Vacutainer tubes (Becton Dickinson). Portions of the liver (median lobe) were minced and placed in RNAlater Stabilization Solution (Applied Biosystems) for gene expression analysis. Sections from the left and median lobes were fixed in 10% neutral buffered formalin followed by 70% ethanol. Paraffin-embedded blocks were sectioned (5 μm) and stained with hematoxylin and eosin (H&E). Histopathological examination was performed by a board-certified veterinary pathologist. Severity scores were assigned for centrilobular degeneration and necrosis (+1, minimal; +2, mild; +3, moderate; +4, marked). Degeneration was defined as prenecrotic hepatocellular change in centrilobular areas, including cytoplasmic hypereosinophilia, nuclear condensation, and cellular dissociation. Degeneration is assumed to precede fulminant necrosis such that, if given more time, degenerating cells likely would have progressed to necrosis. Necrosis was marked by areas of complete hepatocellular destruction and neutrophil infiltration.

Plasma Isolation and Plasma-Derived Exosome Enrichment

Within 15 min of collection, blood was centrifuged to obtain cell-free plasma. ALT activity in fresh plasma was determined using a CLC 720 clinical chemistry analyzer (Carolina Liquid Chemistries). Additional aliquots of plasma were frozen at −80°C until exosome isolation. Thawed plasma was treated with Purified Thrombin Plasma Reagent and exosomes were isolated with ExoQuick Exosome Precipitation Solution (System Biosciences) according to the manufacturer's instructions. The post-ExoQuick supernatant was reserved for RNA isolation to analyze liver-specific RNAs in the extra-exosomal, protein-rich plasma fraction.

Primary Hepatocyte Culture and Medium-Derived Exosome Enrichment

Freshly isolated primary hepatocytes from human donors ($n = 7$; Table 1) and male SD rats ($n = 3$) were obtained from commercial sources (QPS Hepatic Biosciences and Triangle Research Labs).

TABLE 1. Characteristics of primary human hepatocyte donors

Age (year)	BMI	Sex	Race
<1	15	M	African-American
3	17	M	Caucasian
14	24	F	Caucasian
26	32	M	Caucasian
30	33	F	African-American
48	24	F	Caucasian
74	23	F	Caucasian

Individual batches of fresh hepatocytes were seeded into 12-well plates coated with collagen type I (Corning) at a density of 0.9×10^6 cells per well in hepatocyte plating medium (William's E medium, penicillin-streptomycin, GlutaMax, HEPES, sodium pyruvate, fetal bovine serum [Thermo Fisher Scientific], insulin, and dexamethasone [Sigma-Aldrich]). Culture plates were incubated at 37°C with 5% CO_2. After attachment, nonadherent cells were removed and fresh plating medium was added. Cultures were transitioned to hepatocyte maintenance medium without fetal bovine serum after 3–4 h. Following a 24-h acclimation period, hepatocyte cultures were exposed to APAP or a medium control (vehicle) for 24 h. All conditions were tested in triplicate culture wells for each rat or human donor.

Hepatocyte-conditioned medium (1–2 ml) was collected after 24 h and clarified by centrifugation at 3000 *g* for 15 min. Exosomes were precipitated from medium with ExoQuick-TC (System Biosciences) following the protocol for this sample type. Lactate dehydrogenase (LDH) activity was assayed with a Cytotoxicity Detection Kit (Roche) as described previously in Kia *et al.* (2015). Cellular ATP content was measured with CellTiter-Glo Luminescent Cell Viability Assay (Promega) according to the manufacturer's instructions. Data were collected using a SpectraMax M3 microplate reader (Molecular Devices).

EV Characterization and Validation of Exosome Enrichment

Nanoparticle tracking analysis

Nanoparticle tracking analysis was performed on exosomes produced *in vitro* using a NanoSight NS500 (Malvern Instruments). The instrument was calibrated using polystyrene bead standards (100 nm) before each use (Malvern Instruments). Diluted samples were advanced through the detection chamber to obtain 5 readings per sample, each with a capture period of 60 s. Particle concentration and size were determined using NTA software version 3.0 (Malvern Instruments).

Electron microscopy

Exosomes were precipitated from filtered (0.2 μm PES) hepatocyte-conditioned culture medium using ExoQuick-TC. Exosome preparations were diluted 1:1000 in Dulbecco's phosphate buffered saline to start the assembly reaction. At 10 min, samples were applied to glow-discharged 200 mesh Quantifoil R 2/1 grids (Electron Microscopy Sciences), blotted briefly, and plunged into liquid ethane as described previously (Dokland, 2006). The frozen grids were transferred to a Gatan 622 cryo-holder and imaged using an FEI Tecnai F20 transmission electron microscope, operated at 200 kV with magnifications from 5000 to 29 000× and defocus settings of −6.0 to −10.0 μm. Images were collected on a Gatan Ultrascan 4000 CCD camera.

Immunoblot analysis

Protein extracts were prepared from hepatocyte monolayers or exosomes using RIPA Lysis and Extraction Buffer (Thermo) with Halt Protease Inhibitor Single-Use Cocktail (Thermo), and Triton X-100 (hepatocytes only). Protein concentration was determined using the BCA Protein Assay Kit (Thermo). Equal protein quantities of each sample were separated on 4–12% NuPAGE Bis-Tris gels (Life Technologies) and transferred to Immobilon-FL PVDF membranes (Millipore). Membranes were blocked with either 5% (w/v) nonfat dry milk in PBS or Odyssey PBS Blocking Buffer (Licor Biosciences). The following primary antibodies were used for immunoblotting: Flotillin-1 (BD Transduction Laboratories), CD63 (Abcam), CD81 (AbD Serotech), Prohibitin-1 (Santa Cruz Biotechnology Inc.), and Grp78 (BD Transduction Laboratories). Proteins were detected using IRDye secondary antibodies (Licor Biosciences) or Alexa Fluor 680-conjugated AffiniPure IgG (Jackson Immunoresearch Laboratories). Blots were imaged using an Odyssey Classic Imaging System (Licor Biosciences).

Total RNA Isolation and Analysis by Absolute qRT-PCR

Total RNA was isolated from plasma- and culture medium-derived exosomes using the miRCURY Cell & Plant Isolation Kit (Exiqon) according to the manufacturer's instructions for RNA isolation from blood. To analyze extracellular RNA in the protein-rich compartment of culture medium and plasma, total RNA was isolated from culture medium samples or post-ExoQuick plasma supernatants, respectively, using the miRNeasy Serum/Plasma Kit (Qiagen) and manufacturer's protocol. Total RNA from rat liver, rat hepatocytes, and human hepatocytes was isolated with the miRNeasy Mini Kit (Qiagen) according to the manufacturer's instructions. For all RNA isolations, a spike-in cocktail consisting of linear acrylamide carrier (Applied Biosystems) and exogenous RNA controls, Luciferase mRNA mimic (Promega) and *Caenorhabditis elegans* miR-39 (Qiagen), was added.

Synthesis of cDNA for mRNA analysis was performed with equal volumes of RNA using a High-Capacity cDNA Reverse Transcription Kit (Applied Biosystems). RT-PCR was performed on a 7900HT Fast RT-PCR System (Applied Biosystems) using TaqMan Gene Expression Assays and Fast Advanced Master Mix. Absolute quantities of mRNAs were calculated using a species-matched standard curve generated from bacterial plasmids or PCR amplification of liver cDNA. Synthesis of cDNA for analysis of miR-122 copy number was performed using a TaqMan miRNA Reverse Transcription Kit (Applied Biosystems). Absolute qRT-PCR was performed on a 7900HT Fast RT-PCR System (Applied Biosystems) using TaqMan miRNA Assays (hsa-mir-122-5p) and Universal Master Mix II (no UNG). Absolute quantities of miR-122 in cells, exosomes, and the protein-rich fraction were computed from a standard curve of synthetic miR-122 cDNA.

Statistical Analysis

Analyses were conducted using GraphPad Prism 6 (GraphPad Software, Inc.) unless otherwise noted. For all tests, $p < 0.05$ was considered statistically significant. Mean values from plasma-based endpoints (i.e. exosomal RNA and ALT activity) were analyzed using a 2-way analysis of variance (ANOVA). Results from APAP-treated animals were compared with time-matched control groups with Fisher's Least Significant Difference (Fisher's LSD) test. *In vitro* data from rat hepatocytes were averaged across triplicate wells and a fold change relative to control was calculated for each rat. Fold changes across rats ($n = 3$) were averaged and compared by 1-way ANOVA. Results from each

APAP concentration were compared with controls using Dunnett's test for multiple comparisons. *In vitro* data from each human hepatocyte batch were averaged across triplicate wells and a fold change relative to donor-matched controls was calculated. From individual fold changes, a mean across all donors was obtained. Mean fold changes of control and APAP-treated groups were compared by Student's 2-tailed *t*-test.

RESULTS

Exosomal Albumin Transcript Quantities Are Significantly Elevated Prior to APAP-Induced Hepatic Necrosis in Rats

Adult male SD rats were administered a low (500 mg/kg) or high (1400 mg/kg) dose of APAP or a vehicle control and were sacrificed at 0, 1, 2, 4, 8, 12, or 24 h post-dose. Liver injury was determined by histology and plasma ALT activity. Liver-specific RNAs isolated from circulating exosomes were quantified to determine the relationship between HDE alterations and liver injury. Histological findings of necrosis (Figs. 1A–D; Supplementary Table 1) and elevated plasma ALT activity (Figure 2A, Supplementary Figure 1A) were observed only in rats treated with the high dose of APAP at 24 h post-exposure. Exosomal albumin transcript (*ALB*) quantity, however, was significantly elevated in APAP-treated animals (relative to time-matched, vehicle-treated controls) prior to histological observations of necrosis or increases in plasma ALT (Figure 2B, Supplementary Figure 1B). Drug-induced elevations in mean exosomal *ALB* quantity were detected as early as 4 h post-dose; these elevations became dose-dependent at 8 h post-dose. By 12 h, mean exosomal *ALB* mRNA had increased 30- and 50-fold in the low- and high-dose groups, respectively (Figure 2B). Increases in exosomal *ALB* reached statistical significance in the high dose group at 12 h and in the low dose group at 24 h, without signs of liver injury (Figure 2B, Supplementary Figure 1B). Together, these data suggest that changes in HDE release occur as a result of subtoxic APAP exposure *in vivo*.

Quantity and Distribution of Extracellular miR-122 Are Altered by Subtoxic APAP Exposure *In Vivo*

Unlike *ALB* mRNA which was not detected outside of the exosomal plasma fraction (data not shown), circulating miR-122 is stable in exosomes and in a 'protein-rich' Argonaute-bound form (Arroyo *et al.*, 2011; Hornby *et al.*, 2014). In order to determine if miR-122 followed a similar trend as exosomal *ALB* upon *in vivo* APAP exposure, we measured exosomal and protein-rich fractions of circulating miR-122. A trend toward increased exosomal miR-122 was observed in APAP-treated animals at 8 h post-dose (Figure 3A, Supplementary Figure 1C). This trend continued, with mean levels reaching 3- and 4-fold over controls in the low- and high-dose groups at 12 h, respectively. At 24 h post-dose, mean exosomal miR-122 quantities in the low-dose group reached 9-fold that of vehicle-treated controls, despite a lack of hepatocellular toxicity. MiR-122 in the protein-rich fraction showed trends similar to exosomal miR-122 but was significantly elevated in the low-dose group after 24 h (Figure 3B, Supplementary Figure 1D). Whereas the content of miR-122 in both exosomal and protein-rich compartments was increased

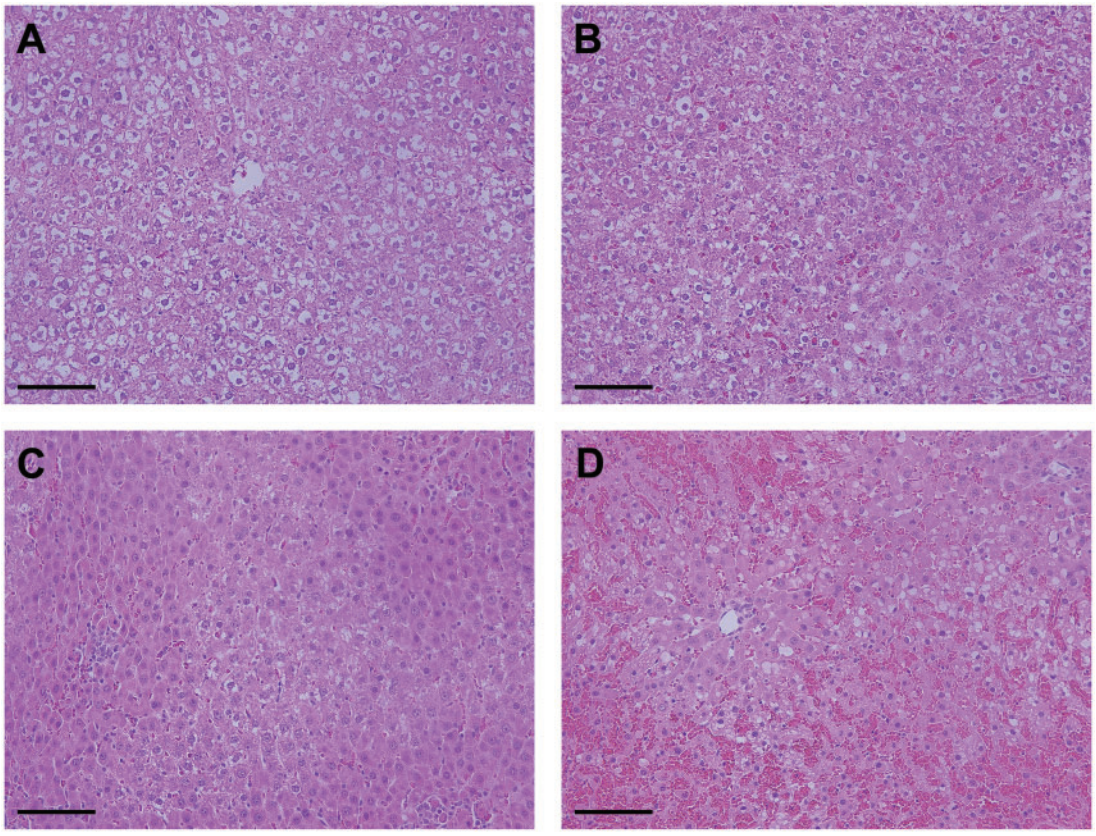

FIG. 1. Histopathology of rat liver sections 24 h after APAP treatment. Representative photomicrographs of H&E stained liver sections from rats 24 h after administration of **(A)** 0.5% methylcellulose vehicle, **(B)** 500 mg/kg APAP, or 1400 mg/kg APAP with **(C)** moderate or **(D)** marked centrilobular necrosis. Bars indicate 200 μm.

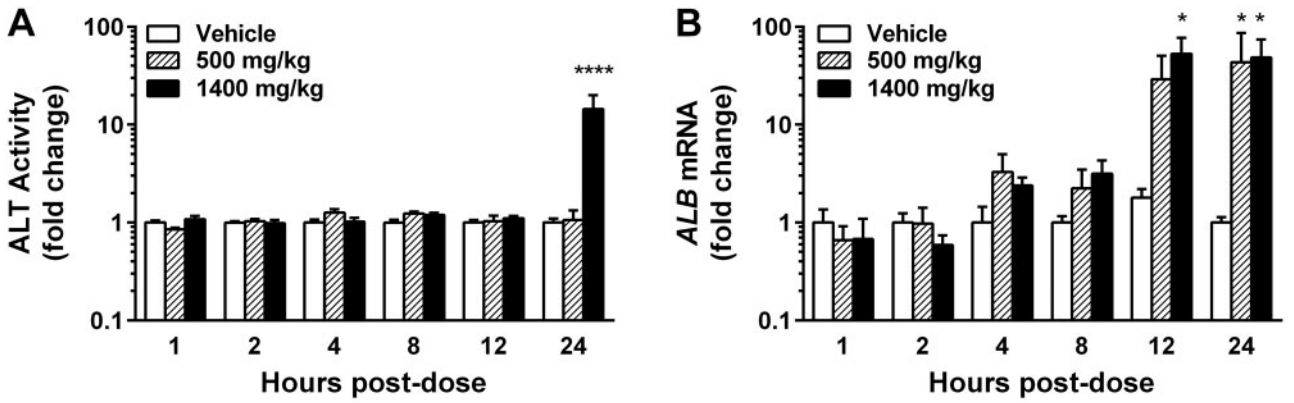

FIG. 2. *In vivo* elevations in ALT activity and exosomal *ALB* as a function of APAP dose and exposure time. APAP-induced elevations in **(A)** plasma ALT activity and **(B)** exosomal *ALB* mRNA. Data are presented as mean + SEM of fold change over time-matched controls ($n = 5$–6 rats/group). $^{*}p < 0.05$, $^{****}p < 0.0001$; 2-way ANOVA with Fisher's LSD.

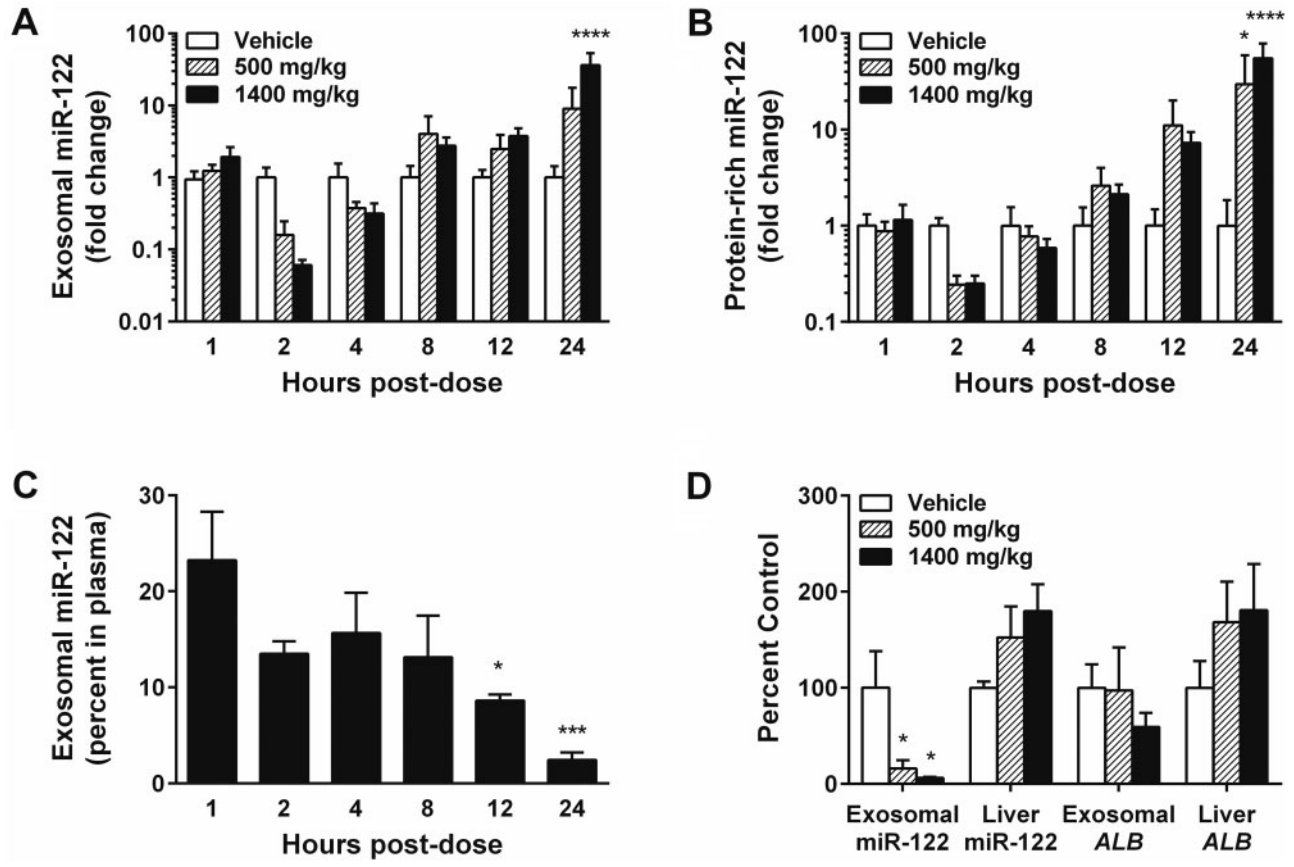

FIG. 3. Alterations in exosomal and protein-rich fractions of miR-122 after *in vivo* APAP exposure. Fold change in **(A)** exosomal and **(B)** protein-rich miR-122 plasma compartments relative to time-matched vehicle controls ($n = 5$–6 rats/group). $^{*}p < 0.05$, $^{****}p < 0.0001$; 2-way ANOVA with Fisher's LSD. **(C)** Percentage of circulating miR-122 in HDE from 1400 mg/kg APAP-treated rats. $^{*}p < 0.05$, $^{***}p < 0.001$; 1-way ANOVA with Dunnett's post-test relative to $t = 1$ h. **(D)** Relationship between liver-specific RNAs measured in exosomes and liver tissue at 2 h post-dose. $^{*}p < 0.05$; 1-way ANOVA with Dunnett's post-test relative to vehicle. Data are presented as mean + SEM.

by APAP exposure in our study, the distribution of miR-122 between these plasma compartments shifted over time. In the high-dose group, the percentage of circulating miR-122 within HDE decreased over time and reached statistical significance at 12 h, prior to overt liver injury (Figure 3C).

Unexpectedly, we observed previously undocumented dose-dependent decreases in exosomal and protein-rich miR-122 fractions after 2 h of APAP exposure, which were not accompanied by decreases in exosomal *ALB* (Figure 3D). To determine whether the decreases in exosomal miR-122 reflected selective packaging of RNA into HDE or decreased hepatocyte miR-122 content, we quantified miR-122 in liver tissue obtained from the 2 h post-exposure animals. There was a trend toward increased hepatic miR-122 copy number

coincident with statistically significant dose-dependent decreases in exosomal miR-122 (Figure 3D). Exosomal *ALB*, however, was not significantly affected in circulating exosomes or liver tissue (Figure 3D).

EV Preparations From Primary Rat and Human Hepatocyte Cultures Are Highly Enriched for Exosomes

We selected a well-characterized exosome enrichment method for our *in vivo* studies, and evidence suggests that most EVs released by hepatocytes are exosomal in size (Giugliano *et al.*, 2015; Koeck *et al.*, 2014; Momen-Heravi *et al.*, 2015a; Royo *et al.*, 2013). However, multiple cell types and tissues contribute to the population of circulating vesicles, and therefore we could not study the nature of hepatocyte-specific vesicles isolated from the *in vivo* samples. To confirm the presence of exosomes in EVs isolated by ExoQuick, we analyzed the size, morphology, and protein enrichment of EVs produced *in vitro* by primary rat and human hepatocytes.

EVs were isolated from conditioned medium of untreated primary rat or human hepatocytes by ExoQuick-TC polymer precipitation. Nanoparticle tracking analysis of rat and human EV preparations revealed a majority of small exosome-sized particles <200 nm in diameter, with the greatest concentration of particles being <100 nm in size (Figs. 4A and B). These results were confirmed using a ZetaView instrument (ParticleMetrix) (data not shown). Cryo-electron microscopy verified exosome enrichment in precipitated rat and human EV preparations, which contained circular membrane-bound vesicles smaller than 100 nm (Figs. 4C and D). Western immunoblot analyses of rat EVs confirmed the presence of exosomal protein markers CD81 and CD63 (Figure 4E). Prohibitin-1, a mitochondrial membrane protein, was detected in rat hepatocytes but was not present in rat HDE, suggesting a lack of cellular contamination in exosomal samples (Figure 4E). Human EV preparations were positive for exosomal markers CD63 and Flotillin-1 and did not contain detectable cellular contamination, as measured by Prohibitin-1 and Grp78, a protein found in the endoplasmic reticulum (Figure 4F). These results confirm that our ExoQuick preparations contain mostly HDE.

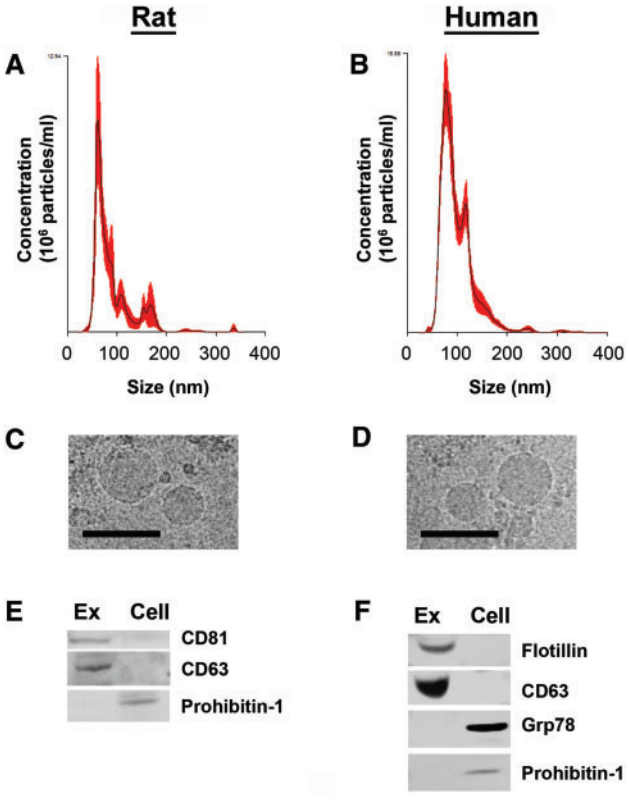

FIG. 4. Characterization of exosome enrichment in EVs secreted by primary rat and human hepatocytes. Representative nanoparticle tracking analyses illustrating the average size distribution (+ SEM) of EVs isolated from untreated **(A)** rat and **(B)** human hepatocyte-conditioned culture medium. Representative cryo-electron micrographs of **(C)** rat and **(D)** human hepatocyte-derived EV preparations. Bars indicate 100 nm. Western blot analysis of exosomal and cellular markers in **(E)** rat and **(F)** human HDE ('Ex') relative to hepatocytes ('Cell').

Subtoxic APAP Exposure Elicits Exosomal RNA Elevations in Primary Rat Hepatocytes

To further characterize HDE release from drug-treated hepatocytes, we explored whether APAP-dependent changes in exosomal RNA content observed *in vivo* could be reproduced in monocultures of primary rat hepatocytes. Primary rat hepatocytes were exposed to a concentration range of APAP (0–30 mM) for 24 h. Across 3 rat hepatocyte batches, statistically significant elevations in LDH leakage and decreases in cellular ATP were not observed at concentrations <30 mM APAP (Figure 5A). However, statistically significant increases in exosomal *ALB* mRNA were evident at concentrations as low as 1.1 mM APAP (Figure 5B). Hepatocellular *ALB* levels were not altered significantly at any APAP concentration, suggesting that increased exosomal *ALB* was not a result of increased expression at the cellular level. In contrast to our *in vivo* findings, miR-122 was not elevated significantly in the exosome- or protein-rich fractions prior to the onset of overt cytotoxicity (Figure 5C).

We then tested the hypothesis that liver-specific exosomal RNA levels are indicative of HDE number, which cannot currently be assessed *in vivo*. We performed nanoparticle tracking analysis on HDE from primary rat hepatocyte cultures exposed to 0, 10, or 30 mM APAP for 24 h ($n = 2$ rats). No statistically significant changes in HDE quantity were observed at any concentration (Figure 5D).

Increased Secretion of Exosomal RNA in the Absence of Overt APAP Toxicity Translates to Primary Human Hepatocyte Cultures

To determine whether primary human hepatocytes would respond to APAP exposure by increasing production of exosomal RNAs, we separately exposed individual batches of freshly isolated primary hepatocytes ($n = 7$ donors) to a subtoxic APAP concentration (10 mM) for 24 h (Figure 6A). APAP treatment caused increases in mean exosomal *ALB* (not statistically significant) and miR-122 ($p < 0.001$) levels in the absence of overt injury (Figs. 6B and C). Quantities of *ALB* and miR-122 in cells and protein-rich medium fractions were not affected by APAP exposure (Figs. 6B and C).

To define the relationship between drug-induced changes in liver-specific exosomal RNA and HDE number in a human system, nanoparticle tracking analysis was performed on exosomes isolated from control and treated (0 vs 10 mM APAP) primary human hepatocyte cultures ($n = 4$ donors). As observed in the rat experiments, APAP exposure did not cause statistically significant changes in exosome quantity (Figure 6D).

Establishing Baseline Quantities of Liver-Specific RNAs in Exosomes From Primary Human Hepatocytes

Individual lots of primary human hepatocytes ($n = 7$) were cultured for 24 h with or without 10 mM APAP. Substantial donor-to-donor variability in the exosomal quantities of *ALB* and miR-122 was apparent. To identify donor characteristics that potentially influenced exosomal content, we related characteristics such as sex, age, BMI, and race to the quantity of liver-specific exosomal RNAs from medium control- and APAP-treated hepatocytes (Supplementary Figure 2A). No association reached statistical significance, but we observed a relationship between exosomal *ALB* and BMI ($p = 0.074$, regression analysis) in untreated hepatocytes (Supplementary Figure 2B).

In an effort to establish healthy ranges of exosomal *ALB* and miR-122, we examined absolute copy numbers of these exosomal RNAs across hepatocyte donors ($n = 7$) under control conditions. We found that quantities of exosomal miR-122 generally corresponded with levels of protein-rich miR-122, although this relationship did not hold true for every donor (Supplementary Figure 3A). We did not observe a consistent relationship between exosomal and cellular *ALB*. Absolute copy numbers of exosomal miR-122 ranged from approximately 10^7–10^9, while exosomal *ALB* ranged from approximately 10^3–10^6 (Supplementary Figs. 3A and B).

Additional Liver-Enriched Transcripts Are Present in Human HDEs

Finally we sought to confirm that additional liver-enriched mRNAs previously identified in rat EVs, and enriched in both rat and human liver, were packaged within human HDE (Miyamoto *et al.*, 2008; Okubo *et al.*, 2013; Royo *et al.*, 2013; Yu *et al.*, 2010). Exosomes were precipitated from the culture medium of untreated primary human hepatocytes ($n = 3$ donors), and exosomal transcripts were quantified by absolute qRT-PCR. All 7 liver-enriched transcripts were detected in human HDE under control conditions, and although the absolute amounts varied, the relative proportions of each mRNA across donors were consistent (Figure 7).

DISCUSSION

To determine whether HDE could mediate the immune reactions that occur without overt hepatotoxicity following drug exposure, we tested the hypothesis that HDE content and/or number would be altered by drug-induced hepatocellular stress in the absence of cell death. We found that the RNA content of HDE was affected prior to, and in the absence of, overt hepatocellular injury in rats receiving both toxic and subtoxic doses of APAP. These results translated across experimental models and species as similar phenomena were observed in primary hepatocyte cultures from both rats and humans.

APAP was selected for this work largely for its defined toxicity profile *in vivo* and in cultured hepatocytes from both rats and humans. Although we are ultimately interested in the role of exosomes in immune signaling, this study does not address the consequences of the immune component of APAP-induced hepatotoxicity, a topic that remains controversial. Whether advantageous (Antoniades *et al.*, 2012; Jaeschke *et al.*, 2012; Ju *et al.*, 2002; Williams *et al.*, 2014) or damaging (Fannin *et al.*, 2015; Ferreira *et al.*, 2016; Huebener *et al.*, 2015; Tujios and Fontana, 2011), there is no question that inflammatory and immune responses are associated with APAP-induced hepatotoxicity in

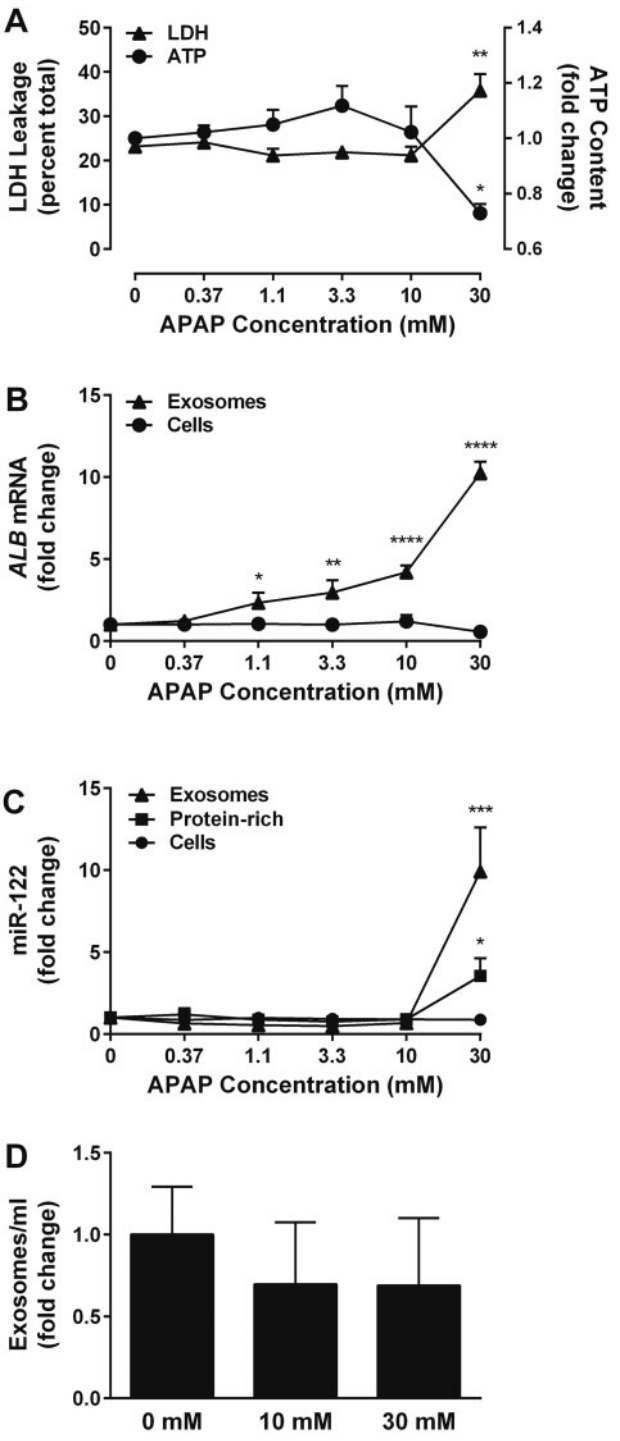

FIG. 5. APAP-induced alterations in exosomes released by primary rat hepatocytes. Data are presented as mean + SEM ($n = 3$ rats) after 24 h APAP exposure. (A) Cytotoxicity, as indicated by cellular ATP and LDH activity in medium. (B) Exosomal and cellular levels of *ALB* in response to APAP. (C) miR-122 in exosomal, protein-rich, and cellular fractions in response to APAP. $^*p < 0.05$, $^{**}p < 0.01$, $^{***}p < 0.001$, $^{****}p < 0.0001$; 1-way ANOVA with Dunnett's post-test relative to vehicle. (D) Nanoparticle tracking analysis on HDE preparations from primary rat hepatocytes ($n = 2$ rats) after 24 h incubation with APAP. Data are presented as the mean + SEM of fold change in exosomes/ml relative to control. No statistically significant differences in exosome quantity between treated and untreated groups were observed; 1-way ANOVA with Dunnett's post-test relative to vehicle.

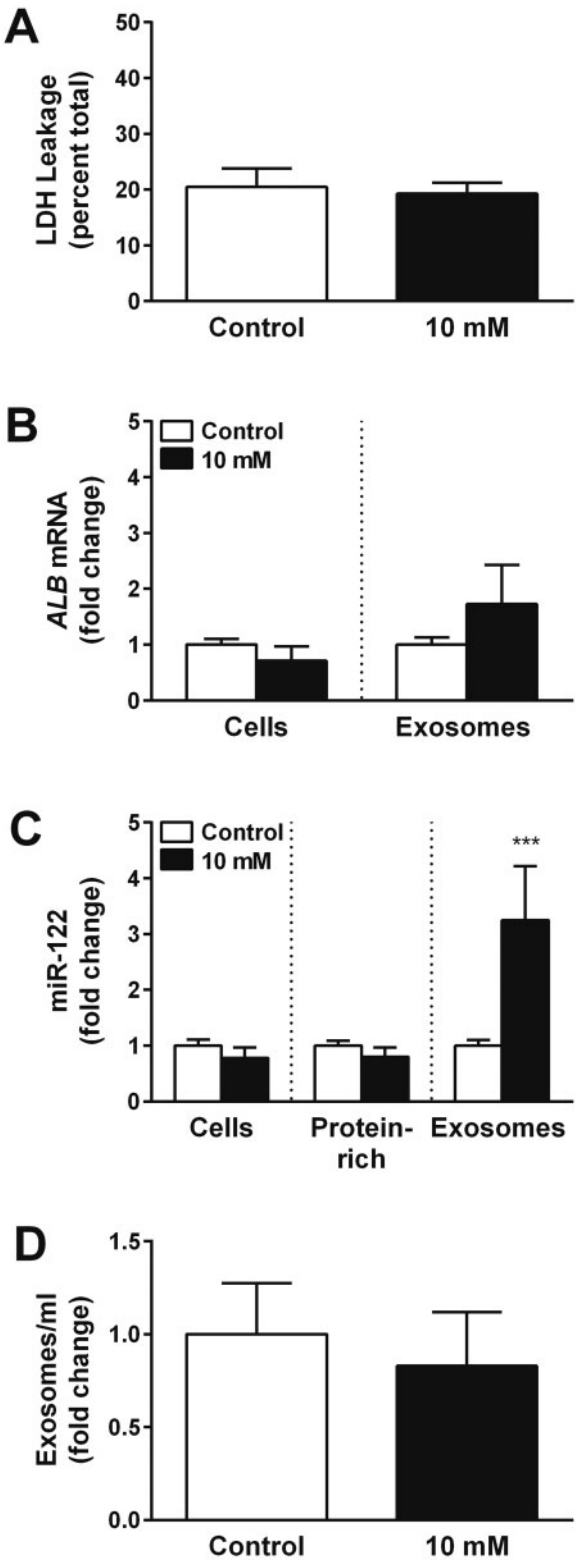

FIG. 6. Alterations in exosomes released by primary human hepatocytes with and without APAP exposure. **(A)** LDH leakage; **(B)** *ALB* mRNA; and **(C)** miR-122 after 24 h of exposure to APAP (10 mM). Data are presented as the mean + SEM across 7 donors. ***$p < 0.001$; Student's *t*-test comparing treatment and control. **(D)** Nanoparticle tracking analysis on HDE preparations from primary human hepatocytes ($n = 4$ donors) after 24 h incubation with APAP. Data are presented as the mean + SEM of fold change in exosomes/ml relative to control. No statistically significant differences in exosome quantity between treated and untreated groups were observed; Student's *t*-test.

humans. In a study of recurrent therapeutic APAP dosing, activation of immune tolerance was evident in the peripheral blood transcriptome of healthy adults without APAP-induced ALT elevations (Fannin *et al.*, 2015). This suggests that immune responses after APAP exposure manifest prior to overt hepatocellular injury, a process that likely involves subtoxic hepatocellular release of stress signals such as HDE.

Although mouse models are generally considered to be more appropriate for the study of APAP-induced hepatotoxicity mechanisms (Jaeschke *et al.*, 2014; McGill *et al.*, 2012), the goal of the current work was to evaluate early changes in HDE that occur during APAP-induced stress, prior to hepatocellular injury. Therefore, the rat was intentionally selected as a relatively resistant preclinical species to extend the duration of APAP-induced stress *in vivo* so that HDE alterations could be observed prior to overt DILI. Evidence suggests that this latency may be more similar to humans than the latency to fulminant hepatotoxicity observed in mice (Jaeschke *et al.*, 2014). Because mouse hepatocytes are difficult to culture, selection of a rat model also facilitated comparisons of data collected from primary hepatocytes relative to *in vivo* data from the same species.

In this study, we selected liver-specific exosomal contents *ALB* mRNA and miR-122 as translational markers of HDE alteration that also elicit immunologically relevant responses when transferred to other cell types (Momen-Heravi *et al.*, 2015a; Royo *et al.*, 2013). Circulating *ALB* mRNA and miR-122 have been identified previously as more sensitive and specific biomarkers of liver injury in both preclinical species and humans (Antoine *et al.*, 2013; Okubo *et al.*, 2013; Starckx *et al.*, 2013; Wang *et al.*, 2009; Zhang *et al.*, 2014). In particular, the value of miR-122 in peripheral blood as a biomarker of APAP overdose is well established (Antoine *et al.*, 2013). Therefore, the biomarker potential of miR-122 and HDE was not a focus of this work.

In our *in vivo* rat model of APAP-induced liver injury, the proportion of plasma miR-122 contained within exosomes decreased over time in the high-dose group, presumably as a function of increased hepatocellular damage. These data are in agreement with what is known about the active nature of exosome release and the passive, necrotic release of protein-rich miR-122 (Bobrie *et al.*, 2011; Dear and Antoine, 2014; Kia *et al.*, 2015; Turchinovich *et al.*, 2011, 2013; Villarroya-Beltri *et al.*, 2014). Similar shifts in miRNA localization between protein-rich and exosomal fractions have been observed in DILI, and the nature of these shifts may reflect different mechanisms of liver injury (Bala *et al.*, 2012, 2015). We propose that shifts in miRNA localization, such as those shown here, may serve a biological signaling purpose. For example, miR-122 in HDE released by alcohol-treated hepatocytes can prime monocytes for activation, while biological activity has yet to be attributed to miRNA in the protein-rich form (Momen-Heravi *et al.*, 2015a; Turchinovich *et al.*, 2013). Similarly, the effects of inflammatory mediators such as Hsp70 are amplified when they are delivered to recipient cells via exosomes (De Maio, 2011). While it is unlikely that exosomal miR-122 is a driving factor or major inflammatory mediator in overt APAP hepatotoxicity, during which necrosis releases massive amounts of DAMPs, the present miR-122 results support the assertion that HDE alterations may be actively mediated and functionally relevant in the early stages of hepatocyte stress.

In vivo, parallel increases in HDE-associated *ALB* mRNA and miR-122 were generally observed. However, exosomal *ALB* mRNA did not decrease *in vivo* at early time points alongside exosomal miR-122, providing evidence for the selective packaging of RNA into HDE. Selective mRNA packaging into exosomes

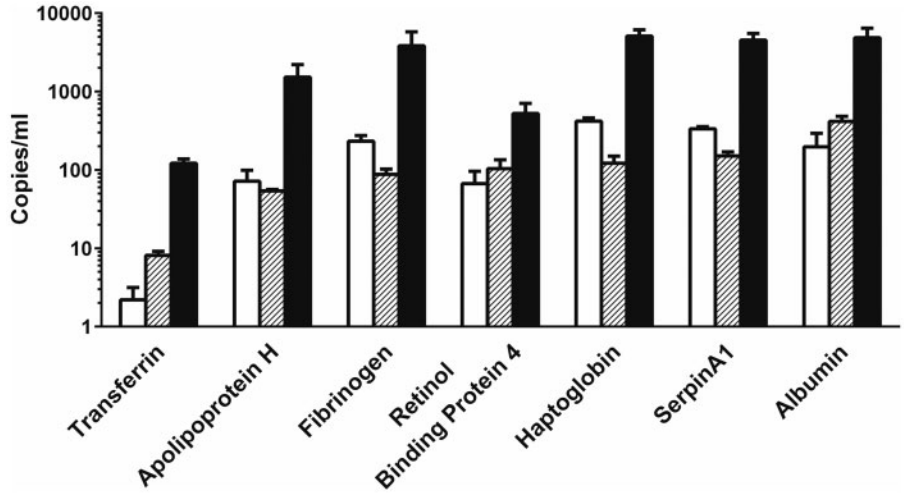

FIG. 7. Analysis of additional liver-enriched transcripts within exosomes released by untreated primary human hepatocytes. Bars denote different donors ($n = 3$). Data represent the mean + SEM of exosomal mRNAs across triplicate culture wells for each donor. Transcript quantities are expressed as exosomal copy number per ml of culture medium used to isolate HDE.

has been observed in circulating vesicles from rats treated with APAP or D-(+)-galactosamine (DGAL), which contained distinct transcript profiles suggestive of compound-specific exosomal content (Wetmore *et al.*, 2010). We confirmed these results with HDE, as different trends in exosomal *ALB* mRNA and miR-122 were observed following APAP and DGAL exposures in primary rat hepatocytes (Supplementary Figure 4). Although subtoxic concentrations of DGAL elicited increases in both exosomal RNAs, neither reached statistical significance prior to overt cytotoxicity. Our nanoparticle tracking results also recapitulate the selective packaging hypothesis by indicating that the quantity of exosomal RNA does not correspond to HDE number. As such, the APAP-induced exosomal *ALB* mRNA elevations observed *in vivo* and *in vitro* are likely the result of increased *ALB* packaging within a similar number of HDE rather than an increase in overall HDE production with constant *ALB* mRNA content. Although these findings are novel, it is important to note that exosome quantification could be affected by the stability of HDE in culture, which is currently unknown. Future experiments to establish the half-life and clearance rate of HDE will be imperative for understanding the biological implications of HDE in DILI.

Although the intent of this work was not to study biomarkers, by defining the kinetics and dose-dependence of HDE release prior to overt DILI, this study could help to validate HDE as sensitive, translational, and clinically relevant biomarkers of DILI. We assayed 7 liver-enriched transcripts within primary human HDE from 3 separate donors. To our knowledge, this is the first characterization of the mRNA content of HDE from primary human hepatocytes. All 7 liver-enriched transcripts were measurable, and there was some consistency in the relative abundance of each transcript across the 3 donors, suggesting that these mRNAs, originally detected in rat HDE (Miyamoto *et al.*, 2008; Okubo *et al.*, 2013; Royo *et al.*, 2013), may also be used to identify human HDE. In addition, we have begun to define normal levels of exosomal *ALB* mRNA and miR-122 across donors. Despite the small donor pool, potential relationships were identified between donor characteristics and exosomal content. Continuing to study donor characteristics that influence HDE RNA content and to define a healthy range of HDE-based RNA levels will be important for interpreting biomarker data in the future. These data will need to be considered in the context of disease, which is known to affect basal HDE quantity and content. For instance, recent evidence suggests that high hepatocellular lipid content and nonlcoholic fatty liver disease correspond to increased EV production by hepatocytes (Hirsova *et al.*, 2016; Kakazu *et al.*, 2015).

In summary, we detected significant alterations in the liver-specific RNA content of HDE at subtoxic doses of the prototypical hepatotoxicant APAP in rats and in primary rat and human hepatocytes. These alterations appear to reflect differential packaging of select RNAs in HDE rather than HDE number. The changes in HDE content observed prior to and in the absence of overt hepatocellular injury, together with growing data on the role of exosomes in stimulating immune responses, support the hypothesis that HDE released from drug-stressed hepatocytes may transmit signals that mediate critical early immune responses across multiple forms of DILI. While this hypothesis was substantiated using an intrinsic hepatotoxicant, future work will address the release kinetics and signaling potential of HDE released by hepatocytes exposed to idiosyncratic DILI compounds.

SUPPLEMENTARY DATA

Supplementary data are available online at http://toxsci.oxfordjournals.org/.

AKNOWLEDGMENTS

We extend our gratitude to J. Scott Eaddy for his contributions to the *in vivo* work described here, including clinical chemistry analysis. We would like to thank Cynthia Rodenburg and Dr. Terje Dokland of the Department of Microbiology Cryo-EM facility at the University of Alabama Birmingham for their assistance with electron microscopy. We also wish to thank Dr. Nazar Filonov, of the Nanomedicine Characterization core facility at the Center for Nanotechnology in Drug Delivery at the University of North Carolina Chapel Hill, for his contributions to nanoparticle tracking analyses.

FUNDING

This work was supported in part by the National Center for Advancing Translational Sciences (NCATS), National Institutes of Health (5UL1TR001111). N.S.H. was supported in part by the National Institutes of Health, National Institute of Environmental Health Sciences (NIEHS) Toxicology Training Grant (T32-ES007126). The content is solely the responsibility of the authors and does not necessarily represent the official views of the National Institutes of Health.

REFERENCES

Adams, D. H., Ju, C., Ramaiah, S. K., Uetrecht, J., and Jaeschke, H. (2010). Mechanisms of immune-mediated liver injury. *Toxicol. Sci.* **115**, 307–321.

Antoine, D. J., Dear, J. W., Starkey Lewis, P., Platt, V., Coyle, J., Masson, M., Thanacoody, R. H., Gray, A. J., Webb, D. J., Moggs, J. G., *et al.* (2013). Mechanistic biomarkers provide early and sensitive detection of acetaminophen-induced acute liver injury at first presentation to hospital. *Hepatology* **58**, 777–787.

Antoine, D. J., Harrill, A. H., Watkins, P. B., and Park, B. K. (2014). Safety biomarkers for drug-induced liver injury – current status and future perspectives. *Toxicol. Res.* **3**, 75–85.

Antoniades, C. G., Quaglia, A., Taams, L. S., Mitry, R. R., Hussain, M., Abeles, R., Possamai, L. A., Bruce, M., McPhail, M., Starling, C., *et al.* (2012). Source and characterization of hepatic macrophages in acetaminophen-induced acute liver failure in humans. *Hepatology* **56**, 735–746.

Arroyo, J. D., Chevillet, J. R., Kroh, E. M., Ruf, I. K., Pritchard, C. C., Gibson, D. F., Mitchell, P. S., Bennett, C. F., Pogosova-Agadjanyan, E. L., Stirewalt, D. L., *et al.* (2011). Argonaute2 complexes carry a population of circulating microRNAs independent of vesicles in human plasma. *Proc. Natl. Acad. Sci. U.S.A.* **108**, 5003–5008.

Bala, S., Csak, T., Momen-Heravi, F., Lippai, D., Kodys, K., Catalano, D., Satishchandran, A., Ambros, V., and Szabo, G. (2015). Biodistribution and function of extracellular miRNA-155 in mice. *Sci. Rep.* **5**, 10721.

Bala, S., Petrasek, J., Mundkur, S., Catalano, D., Levin, I., Ward, J., Alao, H., Kodys, K., and Szabo, G. (2012). Circulating microRNAs in exosomes indicate hepatocyte injury and inflammation in alcoholic, drug-induced, and inflammatory liver diseases. *Hepatology* **56**, 1946–1957.

Bandiera, S., Pfeffer, S., Baumert, T. F., and Zeisel, M. B. (2015). miR-122–a key factor and therapeutic target in liver disease. *J. Hepatol.* **62**, 448–457.

Beninson, L. A., and Fleshner, M. (2014). Exosomes: an emerging factor in stress-induced immunomodulation. *Semin. Immunol.* **26**, 394–401.

Bernal, W., Auzinger, G., Dhawan, A., and Wendon, J. (2010). Acute liver failure. *Lancet* **376**, 190–201.

Bobrie, A., Colombo, M., Raposo, G., and Thery, C. (2011). Exosome secretion: molecular mechanisms and roles in immune responses. *Traffic* **12**, 1659–1668.

Conde-Vancells, J., Rodriguez-Suarez, E., Embade, N., Gil, D., Matthiesen, R., Valle, M., Elortza, F., Lu, S. C., Mato, J. M., and Falcon-Perez, J. M. (2008). Characterization and comprehensive proteome profiling of exosomes secreted by hepatocytes. *J. Proteome Res.* **7**, 5157–5166.

De Maio, A. (2011). Extracellular heat shock proteins, cellular export vesicles, and the Stress Observation System: a form of communication during injury, infection, and cell damage. *Cell Stress Chaperones* **16**, 235–249.

Dear, J. W., and Antoine, D. J. (2014). Stratification of paracetamol overdose patients using new toxicity biomarkers: current candidates and future challenges. *Exp. Rev. Clin. Pharmacol.* **7**, 181–189.

Dokland, T. (2006). Electron microscopy of biological samples. In *Techniques in Microscopy for Biomedical Applications* (T. Dokland, D. W. Hutmacher, M. L. Ng, J. T. Schantz, Eds.). World Scientific Press, Singapore.

Dreux, M., Garaigorta, U., Boyd, B., Decembre, E., Chung, J., Whitten-Bauer, C., Wieland, S., and Chisari, F. V. (2012). Short-range exosomal transfer of viral RNA from infected cells to plasmacytoid dendritic cells triggers innate immunity. *Cell Host Microbe* **12**, 558–570.

Fannin, R. D., Gerrish, K., Sieber, S. O., Bushel, P. R., Watkins, P. B., and Paules, R. S. (2016). Blood transcript immune signatures distinguish a subset of people with elevated serum ALT from others given acetaminophen. *Clin. Pharmacol. Ther.* **99**, 432–441.

Ferreira, D. W., Goedken, M. J., Rommelaere, S., Chasson, L., Galland, F., Naquet, P., and Manautou, J. E. (2016). Enhanced hepatotoxicity by acetaminophen in Vanin-1 knockout mice is associated with deficient proliferative and immune responses. *Biochim. Biophys. Acta* **1862**, 662–669.

Fontana, R. J. (2014). Pathogenesis of idiosyncratic drug-induced liver injury and clinical perspectives. *Gastroenterology* **146**, 914–928.

Giugliano, S., Kriss, M., Golden-Mason, L., Dobrinskikh, E., Stone, A. E., Soto-Gutierrez, A., Mitchell, A., Khetani, S. R., Yamane, D., Stoddard, M., *et al.* (2015). Hepatitis C virus infection induces autocrine interferon signaling by human liver endothelial cells and release of exosomes, which inhibits viral replication. *Gastroenterology* **148**, 392–402 e13.

Hirsova, P., Ibrahim, S. H., Krishnan, A., Verma, V. K., Bronk, S. F., Werneburg, N. W., Charlton, M. R., Shah, V. H., Malhi, H., and Gores, G. J. (2016). Lipid-induced signaling causes release of inflammatory extracellular vesicles from hepatocytes. *Gastroenterology* **pii**, S0016–S5085.

Hornby, R. J., Starkey Lewis, P., Dear, J., Goldring, C., and Park, B. K. (2014). MicroRNAs as potential circulating biomarkers of drug-induced liver injury: key current and future issues for translation to humans. *Exp. Rev. Clin. Pharmacol.* **7**, 349–362.

Huebener, P., Pradere, J. P., Hernandez, C., Gwak, G. Y., Caviglia, J. M., Mu, X., Loike, J. D., Jenkins, R. E., Antoine, D. J., and Schwabe, R. F. (2015). The HMGB1/RAGE axis triggers neutrophil-mediated injury amplification following necrosis. *J. Clin. Invest.* **125**, 539–550.

Hussaini, S. H., and Farrington, E. A. (2014). Idiosyncratic drug-induced liver injury: an update on the 2007 overview. *Exp. Opin. Drug Saf.* **13**, 67–81.

Jaeschke, H., Williams, C. D., Ramachandran, A., and Bajt, M. L. (2012). Acetaminophen hepatotoxicity and repair: the role of sterile inflammation and innate immunity. *Liver Int.* **32**, 8–20.

Jaeschke, H., Xie, Y., and McGill, M. R. (2014). Acetaminophen-induced liver injury: From animal models to humans. *J. Clin. Trans. Hepatol.* **2**, 153–161.

Ju, C., and Reilly, T. (2012). Role of immune reactions in drug-induced liver injury (DILI). *Drug Metab. Rev.* **44**, 107–115.

Ju, C., Reilly, T. P., Bourdi, M., Radonovich, M. F., Brady, J. N., George, J. W., and Pohl, L. R. (2002). Protective role of Kupffer cells in acetaminophen-induced hepatic injury in mice. *Chem. Res. Toxicol.* **15**, 1504–1513.

Kakazu, E., Mauer, A. S., Yin, M., and Malhi, H. (2015). Hepatocytes release ceramide-enriched pro-inflammatory

extracellular vesicles in an IRE1alpha-dependent manner. *J. Lipid Res*. **57**, 233–245.

Kia, R., Kelly, L., Sison-Young, R. L., Zhang, F., Pridgeon, C. S., Heslop, J. A., Metcalfe, P., Kitteringham, N. R., Baxter, M., Harrison, S., *et al*. (2015). MicroRNA-122: a novel hepatocyte-enriched in vitro marker of drug-induced cellular toxicity. *Toxicol. Sci*. **144**, 173–185.

Koeck, E. S., Iordanskaia, T., Sevilla, S., Ferrante, S. C., Hubal, M. J., Freishtat, R. J., and Nadler, E. P. (2014). Adipocyte exosomes induce transforming growth factor beta pathway dysregulation in hepatocytes: A novel paradigm for obesity-related liver disease. *J. Surg. Res*. **192**, 268–275.

Liu, S., Stolz, D. B., Sappington, P. L., Macias, C. A., Killeen, M. E., Tenhunen, J. J., Delude, R. L., and Fink, M. P. (2006). HMGB1 is secreted by immunostimulated enterocytes and contributes to ctyomix-induced hyperpermeability of Caco-2 monolayers. *Am. J. Physiol. Cell Physiol*. **290**, C990–C992.

McGill, M. R., Williams, C. D., Xie, Y., Ramachandran, A., and Jaeschke, H. (2012). Acetaminophen-induced liver injury in rats and mice: comparison of protein adducts, mitochondrial dysfunction, and oxidative stress in the mechanism of toxicity. *Toxicol. Appl. Pharmacol*. **264**, 387–394.

Miyamoto, M., Yanai, M., Ookubo, S., Awasaki, N., Takami, K., and Imai, R. (2008). Detection of cell-free, liver-specific mRNAs in peripheral blood from rats with hepatotoxicity: a potential toxicological biomarker for safety evaluation. *Toxicol. Sci*. **106**, 538–545.

Momen-Heravi, F., Bala, S., Kodys, K., and Szabo, G. (2015a). Exosomes derived from alcohol-treated hepatocytes horizontally transfer liver specific miRNA-122 and sensitize monocytes to LPS. *Sci. Rep*. **5**, 9991.

Momen-Heravi, F., Saha, B., Kodys, K., Catalano, D., Satishchandran, A., and Szabo, G. (2015b). Increased number of circulating exosomes and their microRNA cargos are potential novel biomarkers in alcoholic hepatitis. *J. Trans. Med*. **13**, 261.

Okubo, S., Miyamoto, M., Takami, K., Kanki, M., Ono, A., Nakatsu, N., Yamada, H., Ohno, Y., and Urushidani, T. (2013). Identification of novel liver-specific mRNAs in plasma for biomarkers of drug-induced liver injury and quantitative evaluation in rats treated with various hepatotoxic compounds. *Toxicol. Sci*. **132**, 21–31.

Ostapowicz, G., Fontana, R. J., Schiodt, F. V., Larson, A., Davern, T. J., Han, S. H., McCashland, T. M., Shakil, A. O., Hay, J. E., Hynan, L., *et al*. (2002). Results of a prospective study of acute liver failure at 17 tertiary care centers in the United States. *Ann. Intern. Med*. **137**, 947–954.

Robbins, P. D., and Morelli, A. E. (2014). Regulation of immune responses by extracellular vesicles. *Nat. Rev. Immunol*. **14**, 195–208.

Royo, F., and Falcon-Perez, J. M. (2012). Liver extracellular vesicles in health and disease. *J. Extracell Vesicles* **1**.

Royo, F., Schlangen, K., Palomo, L., Gonzalez, E., Conde-Vancells, J., Berisa, A., Aransay, A. M., and Falcon-Perez, J. M. (2013). Transcriptome of extracellular vesicles released by hepatocytes. *PloS One* **8**, e68693.

Russmann, S., Kullak-Ublick, G. A., and Grattagliano, I. (2009). Current concepts of mechanisms in drug-induced hepatotoxicity. *Curr. Med. Chem*. **16**, 4041–3053.

Starckx, S., Batheja, A., Verheyen, G. R., Jonghe, S. D., Steemans, K., Dijck, B. V., Singer, M., Bogdan, N., Snoeys, J., Vinken, P., *et al*. (2013). Evaluation of miR-122 and other biomarkers in distinct acute liver injury in rats. *Toxicol. Pathol*. **41**, 795–804.

Tujios, S., and Fontana, R. J. (2011). Mechanisms of drug-induced liver injury: from bedside to bench. *Nat. Rev. Gastroenterol. Hepatol*. **8**, 202–211.

Turchinovich, A., Samatov, T. R., Tonevitsky, A. G., and Burwinkel, B. (2013). Circulating miRNAs: cell-cell communication function? *Front. Genet*. **4**, 119.

Turchinovich, A., Weiz, L., Langheinz, A., and Burwinkel, B. (2011). Characterization of extracellular circulating microRNA. *Nucleic Acids Res*. **39**, 7223–7233.

Uetrecht, J., and Naisbitt, D. J. (2013). Idiosyncratic adverse drug reactions: current concepts. *Pharmacol. Rev*. **65**, 779–808.

Urban, T. J., Daly, A. K., and Aithal, G. P. (2014). Genetic basis of drug-induced liver injury: present and future. *Semin. Liver Dis*. **34**, 123–133.

Villarroya-Beltri, C., Baixauli, F., Gutierrez-Vazquez, C., Sanchez-Madrid, F., and Mittelbrunn, M. (2014). Sorting it out: regulation of exosome loading. *Semin. Cancer Biol*. **28**, 3–13.

Wang, K., Zhang, S., Marzolf, B., Troisch, P., Brightman, A., Hu, Z., Hood, L. E., and Galas, D. J. (2009). Circulating microRNAs, potential biomarkers for drug-induced liver injury. *Proc. Natl. Acad. Sci. U.S.A*. **106**, 4402–4407.

Wetmore, B. A., Brees, D. J., Singh, R., Watkins, P. B., Andersen, M. E., Loy, J., and Thomas, R. S. (2010). Quantitative analyses and transcriptomic profiling of circulating messenger RNAs as biomarkers of rat liver injury. *Hepatology* **51**, 2127–2139.

Wilke, R. A., Lin, D. W., Roden, D. M., Watkins, P. B., Flockhart, D., Zineh, I., Giacomini, K. M., and Krauss, R. M. (2007). Identifying genetic risk factors for serious adverse drug reactions: current progress and challenges. *Nat. Rev. Drug Discov*. **6**, 904–916.

Williams, C. D., Bajt, M. L., Sharpe, M. R., McGill, M. R., Farhood, A., and Jaeschke, H. (2014). Neutrophil activation during acetaminophen hepatotoxicity and repair in mice and humans. *Toxicol. Appl. Pharmacol*. **275**, 122–133.

Yu, Y., Ping, J., Chen, H., Jiao, L., Zheng, S., Han, Z. G., Hao, P., and Huang, J. (2010). A comparative analysis of liver transcriptome suggests divergent liver function among human, mouse and rat. *Genomics* **96**, 281–289.

Zhang, X., Zhang, Z., Dai, F., Shi, B., Chen, L., Zhang, X., Zang, G., Zhang, J., Chen, X., Qian, F., *et al*. (2014). Comparison of circulating, hepatocyte-specific messenger RNA and microRNA as biomarkers of chronic hepatitis B and C. *PloS One* **9**, e92112.